

Ferroelectricity in multiferroic magnetite Fe_3O_4 driven by noncentrosymmetric $\text{Fe}^{2+}/\text{Fe}^{3+}$ charge-ordering: First-principles study

Kunihiko Yamauchi¹, Tetsuya Fukushima¹, and Silvia Picozzi^{1*}

1. *Consiglio Nazionale delle Ricerche - Istituto Nazionale di Fisica della Materia (CNR-INFM),
CASTI Regional Lab., 67100 L'Aquila, Italy*

(Dated: June 2, 2009)

By means of first-principles simulations, we unambiguously show that improper ferroelectricity in magnetite in the low-temperature insulating phase is driven by charge-ordering. An accurate comparison between monoclinic ferroelectric Cc and paraelectric $P2/c$ structures shows that the polarization arises because of “shifts” of electronic charge between octahedral Fe sites, leading to a non-centrosymmetric $\text{Fe}^{2+}/\text{Fe}^{3+}$ charge-ordered pattern. Our predicted values for polarization, in good agreement with available experimental values, are discussed in terms of point-charge dipoles located on selected Fe tetrahedra, pointing to a manifest example of electronic ferroelectricity driven by charge rearrangement.

PACS numbers: Valid PACS appear here

“Improper multiferroics”[1, 2, 3, 4, 5] are attractive multifunctional materials, where magnetism and ferroelectricity are strongly coupled. They can be classified according to different driving forces, which primarily break the spatial inversion symmetry paving the way to ferroelectricity : 1) spin order, 2) charge order (CO) and 3) orbital order. In this letter, we will focus on the second group, where LuFe_2O_4 has emerged as a prototype.[6] However, recently Fe_3O_4 has been also suggested as a ferrimagnet with ferroelectricity being induced by charge-ordering,[7] which would depict magnetite as the first multiferroic known to mankind. Fe_3O_4 shows the well-known first order metal-insulator (Verwey) transition at $T_V \sim 120\text{K}$, below which the crystal structure changes from cubic $Fd3m$ to monoclinic structure and $\text{Fe}^{2+}/\text{Fe}^{3+}$ charge ordering is observed at the Fe B sites in the inverse-spinel AB_2O_4 lattice.[8, 9] Earlier experiments[10] suggested Fe_3O_4 to show a spontaneous polarization at low temperatures, with the structure possibly undergoing a transition from monoclinic to triclinic symmetry[11]. However, up to date the physical mechanism underlying the rising of ferroelectricity is largely unknown. Khomskii[7] has suggested that ferroelectric (FE) polarization is caused by a combination of site-centered and bond-centered charges between $\text{Fe}^{2+}/\text{Fe}^{3+}$ ions in the CO B-site Fe_4 -tetrahedron pattern. His model, based on the structure of Ref.[8] assumes each tetrahedron to show a “3:1” CO arrangement (three Fe^{2+} and one Fe^{3+} ions in a tetrahedron, or viceversa), at variance with Anderson’s criterion,[12] where each tetrahedron shows a “2:2” pattern (two Fe^{2+} and two Fe^{3+} ions). The 2:2 arrangement was found from density functional theory (DFT)[13] on the cubic $Fd3m$ structure, distorted by X_3 phonon mode. Moreover, the 3:1 arrangement was recently obtained within

DFT[13, 14, 15] on a monoclinic $P2/c$ structure. In addition, a mixed CO pattern (25% of 2:2 and 75% of 3:1 tetrahedra) was suggested to occur in a base-centered monoclinic Cc structure[16]. Our DFT results, in agreement with Ref.[16], predict the Cc structure to be the ground state, consistently with recent results from resonant X-ray scattering[17]. As discussed in Ref.[16, 19], the Cc symmetry is stabilized by a delicate balance of different effects: Coulomb repulsion, entropy,[12], Fermi-surface nesting [18] leading to a [001] charge-density wave (CDW),[19] oxygen breathing modes, etc.

Recent experimental data showing real time FE switching in magnetite epitaxial thin films were found to be in good agreement with our DFT calculations for the polarization \mathbf{P} in the Cc FE structure.[21] In this letter, we focus on the proof of charge ordering as the microscopic origin of ferroelectricity in Fe_3O_4 , by comparing two monoclinic $P2/c$ and Cc lattice structures. Since the $P2/c$ structure shows inversion symmetry, the total \mathbf{P} must cancel out, so that at most antiferroelectricity may occur; on the other hand, the Cc structure is ferroelectrically active due to the lack of centrosymmetry.

Electronic structure calculations were performed using the “Vienna *Ab initio* Simulation Package (VASP)”,[23] where the projector-augmented-wave potentials, the generalized gradient approximation to the exchange-correlation potential[24] plus an effective on-site Coulomb interaction U were used.[25] In order to compare the total energies, the FE polarization and other relevant properties, we used - for both paraelectric (PE) $P2/c$ and FE Cc states - the primitive cell of the base-centered monoclinic Cc lattice (with 112 atoms/cell) and experimental lattice parameters[20]. Since the difference in experimental lattice constants between the PE and FE phases is $\sim 0.1\%$, the same lattice parameters in both unit-cells were used. The polarization vector \mathbf{P} is described with the conventional lattice vectors (a, b, c) . Internal atomic coordinates were optimized in both $P2/c$ and Cc , starting from experimental Wyck-

*Electronic address: silvia.picozzi@aquila.infn.it

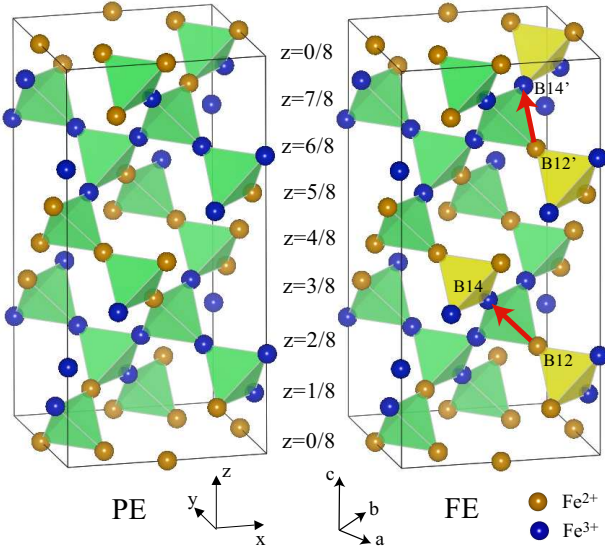


FIG. 1: Ionic structure of Fe octahedral sites in $P2/c$ (left) and Cc (right) cells. Orange and blue balls show Fe^{2+} and Fe^{3+} ions, respectively. Fe_4 tetrahedra of 2:2 and 3:1 CO patterns are highlighted by yellow and green color planes, respectively. Electric dipole moments caused by charge shifts are indicated by red arrows. The lattice vectors in the primitive unit cell (x, y, z) and the conventional cell (a, b, c) are indicated.

off parameters[8, 20]. The conventional atomic positions of the Cc lattice were displaced by $(-1/8, 0, 0)$ to fit into the $P2/c$ structure, so as to have the pseudo-inversion center at $(0, 0, 0)$. We focus on the $P2/c$ and Cc structures since they are both proposed in diffraction experiments[8, 20] and show the lowest DFT total energies compared to other proposed symmetries, *i.e.* $Pmca$ and $Pmc2_1$. [16] Note that the base-centered monoclinic lattice of Cc ($a = b \neq c$, $\alpha \neq \beta \neq \gamma \neq 90^\circ$) is almost identical to a triclinic lattice (experimentally suggested as the FE state), the only difference being the $a = b$ condition. A cutoff energy of 400 eV for plane waves, $4 \times 4 \times 2$ Monkhorst-Pack k -point grid in the Brillouin zone, a threshold of atomic forces of 0.03 eV/Å were used. An effective Coulomb energy $U = 4.5$ eV and an exchange parameter $J = 0.89$ eV (as in Ref.[15]) were used for Fe- d states, although some calculations with different values of U were performed (see below). Fe- $3p^6 3d^6 4s^2$ and O- $2s^2 2p^4$ electrons were treated as valence states. For Fe ions, the ferrimagnetic configuration was considered, with all octahedral Fe sites as up-spin sites and all tetrahedral Fe sites as down-spin sites. Spin-orbit coupling was neglected.

In terms of relevant structural and electronic properties, our results are similar to the previous study by Jeng et. al. [16], so in this letter we will focus only on FE properties. As shown in Fig.1, octahedral Fe sites are located in xy planes with $z = i/8$ ($i=0\dots 7$). The PE state has $\{E, C_{2b} + (0, 0, 1/2), I, \sigma_{2b} + (0, 0, 1/2)\}$ symmetries and the FE state has $\{E, \sigma_{2b} + (0, 0, 1/2)\}$ symmetries

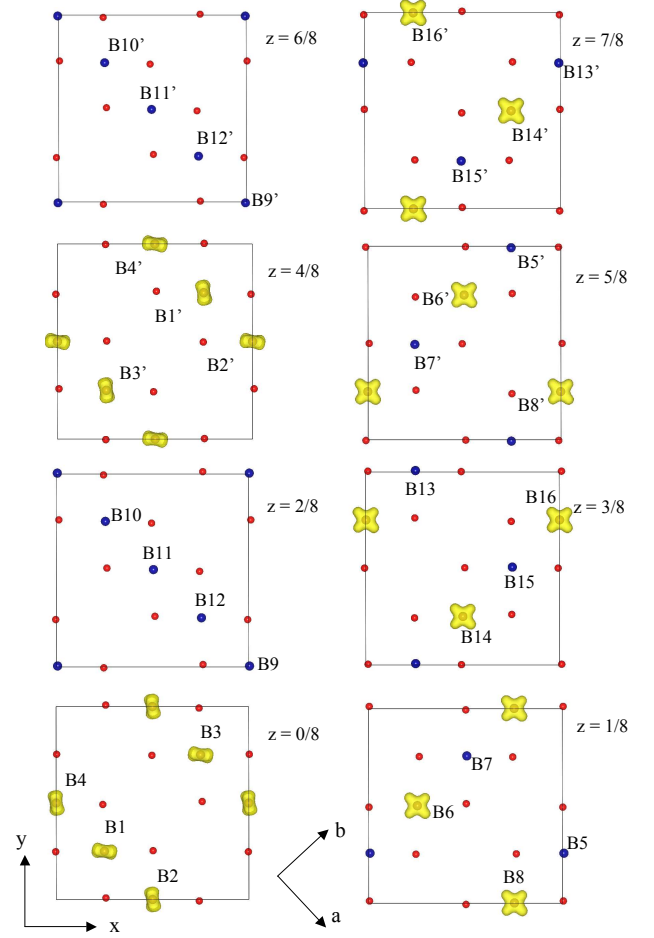


FIG. 2: Charge/orbital ordering of Fe minority t_{2g} states in PE configuration. Blue (orange) large balls show Fe^{3+} (Fe^{2+}) ions. Red small balls show O ions.

in a conventional base centered monoclinic cell so that there are two equivalent atoms (cfr. B12 and B12' sites in Fig.1). Note that *i*) the mirror symmetry along with the translation vector forbids any net polarization along b and finite \mathbf{P} is allowed only along the a and c directions; *ii*) the translation vector is relevant for the CDW stabilization and for opening the energy gap.[19] As discussed in Ref.[15, 16], the PE state shows entirely a 3:1 tetrahedron CO arrangement whereas the FE state shows a mixed pattern. The difference between the two CO distributions (see Fig. 2 for the $P2/c$ and Fig. 3 for the Cc) can be understood when assuming a charge “shift” from B12 to B14 site and, in the upper part of the cell, from B12' to B14', all the other sites keeping their valence state. Each charge shift creates two 2:2 CO tetrahedra, so as to form four 2:2 tetrahedra (cfr. Fig.1). The resulting CO pattern lacks inversion symmetry, therefore allowing FE polarization. The CO rearrangement implies a change in the local breathing mode of O ions, which are driven away (attracted) by the substituted Fe^{2+} (Fe^{3+}) ion at B12 (B14) site, with a displacement of $\sim 0.1\text{\AA}$ (cfr small black arrows in Fig. 3). Similarly, upon charge

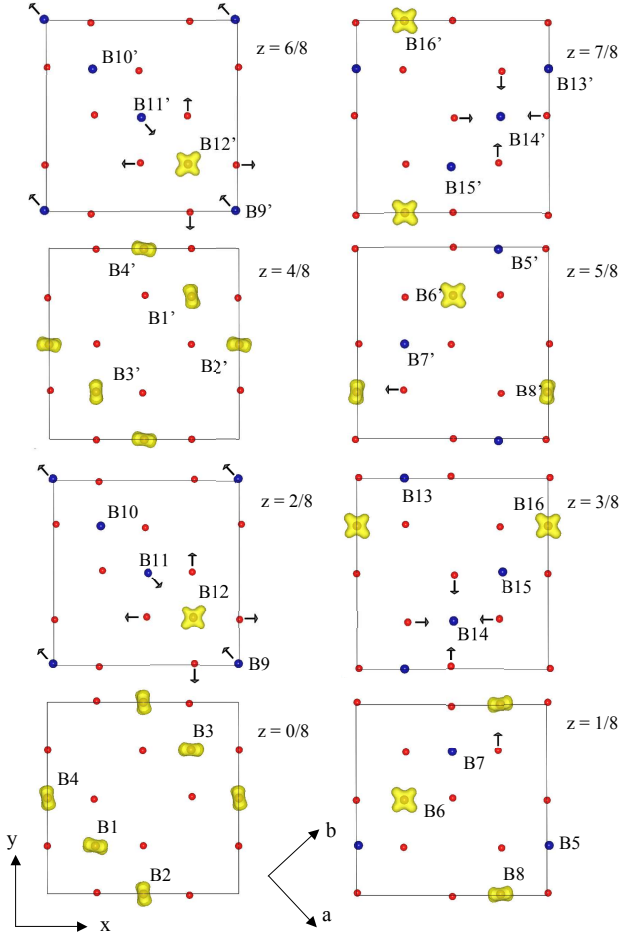


FIG. 3: Charge/orbital ordering of Fe minority t_{2g} states in FE configuration (notation as in Fig.2). Black arrows show atomic displacements with respect to the PE reference state.

shifts of the Fe t_{2g} electron between sites, some of the Fe^{3+} ions (at B9 and B11 sites) move towards the Fe^{2+} ions, maybe reminiscent of Khomskii’s mixed bond-/site-centered charge mechanism.[7] However, as far as ferroelectricity is concerned, when focusing on a Fe chain along [100], these movements average out so as not to give a net contribution to \mathbf{P} .

As for calculated \mathbf{P} (cfr Table I), the Berry phase approach[26] predicts quite a large polarization (at least compared to other improper multiferroics[1, 2]), its direction lying in the ac mirror plane. As noted previously[21], the DFT results are in excellent agreement with recently reported experimental values for magnetite thin films ($P \sim 5.5 \mu\text{C}/\text{cm}^2$ in the ab plane with the c component not measured) as well as with earlier experiments on single crystals[10]: $P_a = 4.8 \mu\text{C}/\text{cm}^2$ and $P_c = 1.5 \mu\text{C}/\text{cm}^2$.

To deepen our analysis, we compare the value of $\mathbf{P}_{\text{Berry}}$ with the value estimated from a point charge model, (\mathbf{P}_{PCM}), assuming the nominal valence for every ion, *i.e.* “full” charge disproportionation, *i.e.* 2+ and 3+ for charge-ordered Fe, 2- for O) as well as with a simple

TABLE I: \mathbf{P} along a , b and c axes (in $\mu\text{C}/\text{cm}^2$), calculated with different approaches (see text).

$\mathbf{P}_{\text{Berry}}$	\mathbf{P}_{PCM}	\mathbf{P}_{dip}
(-4.41, 0, 4.12)	(-4.20, 0, 5.27)	(-4.05, 0, 5.73)

model (\mathbf{P}_{dip}) where we summed up the two dipole moments located at sites where charge-shifting occurs (*i.e.* from B12 to B14 site) with nominally one electron (see red arrows in Fig. 1). The consistency of these values, shown in Table I, implies two important facts: (i) \mathbf{P} is induced largely by the CO rearrangement (*i.e.* charge shifts at few sites) but not much by the ionic displacements, as evident by the similarity between \mathbf{P}_{PCM} and \mathbf{P}_{dip} ; (ii) since the Berry phase value is equivalent to the sum of Wannier-function (WF) centers[26], the similarity between $\mathbf{P}_{\text{Berry}}$ and \mathbf{P}_{PCM} suggests the WF of Fe- d electron to be mostly centered at the ionic sites, no matter how the WF is delocalized and hybridized with surrounding O- p orbitals.

TABLE II: Charge separation (cs, *i.e.* difference of d -charges between Fe^{2+} and Fe^{3+} ions in the atomic sphere with 1Å radius) and the corresponding FE $\mathbf{P}_{\text{Berry}}$ (in $\mu\text{C}/\text{cm}^2$) vs Coulomb repulsion U (J is fixed to 0.89 eV).

U (eV)	4.5	6.0	8.0
cs	0.17	0.23	0.30
$\mathbf{P}_{\text{Berry}}$	(-4.41, 0, 4.12)	(-4.42, 0, 4.81)	(-4.33, 0, 5.07)

Our picture based on the WF centers is also confirmed by the results of $\mathbf{P}_{\text{Berry}}$ values upon varying the U Coulomb parameter. As shown in table II, upon increasing U and keeping the atomic configuration fixed to that obtained for $U = 4.5$ eV, the charge separation between Fe^{2+} and Fe^{3+} is enhanced. Note that the value of \mathbf{P} does not change rapidly with U , suggesting the centers of the WF not to move significantly far from the Fe^{2+} for all U values. Also, in the limit of extremely large U , we expect a “full” charge disproportionation to occur, causing $\mathbf{P}_{\text{Berry}}$ to become progressively closer to \mathbf{P}_{PCM} (as confirmed by Table II).

For further insights, an “adiabatic” path is set up to connect the PE and FE state by displacing all ions linearly with a scaling parameter λ (*i.e.* $\lambda=1$ for full FE displacements and $\lambda=0$ for the initial PE structure). The FE structure with opposite \mathbf{P} was built starting from the PE structure and with $\lambda=-1$, *i.e.* with displacements opposite to the structure considered so far. By analogy with the above discussion for positive λ values, two charge shifts between B10 and B6 (B10’ and B6’) occur as a transition from the PE to the “negative” FE phase. The charge separation (cs) is calculated by comparing the “muffin-tin” charge on the sites where the shift occurs in going from PE to FE (*i.e.* B12 - B14 sites when $\lambda > 0$). The results are reported in Fig.4. The total energy shows a double valley structure, typical for ferroelectric-

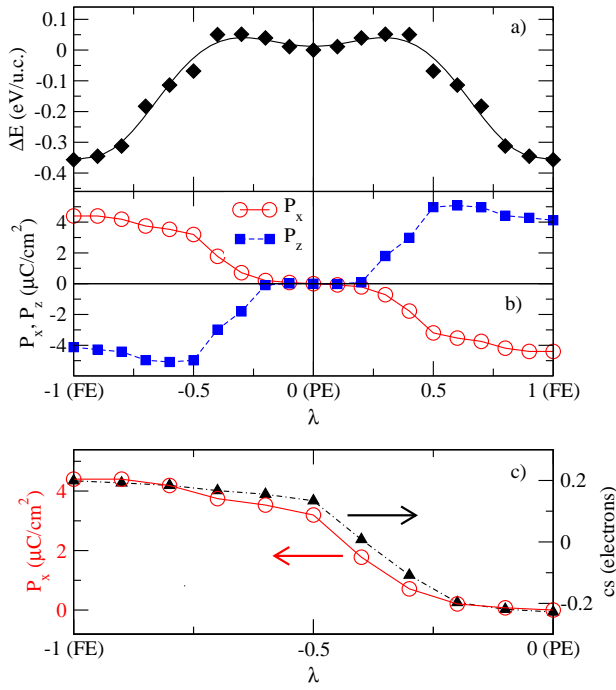


FIG. 4: a) Total energy per unit cell (ΔE , with the black line as a guide to the eye) and b) Polarization (P_x and P_z components) along the adiabatic path between FE structures with opposite \mathbf{P} through the PE structure, vs the scaling parameter λ (see text). c) Polarization P_x (left scale on the y -axis, see empty red circles) and charge separation (right scale on the y -axis and filled black triangles) along the FE ($\lambda = -1$) to PE ($\lambda = 0$) path.

ity, with a deep global minimum at the FE state, along with a very shallow local minimum at the PE state. In going from the PE to the FE state, we show that the charge shift rather suddenly occurs around $\lambda=0.5$, when \mathbf{P} is strongly enhanced and the total energy reduced (cfr. Fig.4 a) and b)). Moreover, the origin of ferroelectricity as driven by charge rearrangements on different sites is clearly confirmed by the trend of P_x closely following that of cs along the path (cfr. Fig.4 c)).

In summary, we have shed light on the microscopic origin of ferroelectric polarization in insulating magnetite by analyzing the differences between two charge-ordered states: the $P2/c$ PE state and the Cc FE state. Ferroelectricity is induced by a non-centrosymmetric charge-ordering and the polarization is primarily caused by local dipoles at selected octahedral sites, pointing to a picture of ferroelectricity mostly based on localized “charge shifts”. Our calculations show that Fe_3O_4 can be considered as a prototypical case of charge-order driving multiferroicity with relatively large values for the electric polarization.

Acknowledgments

We thank Prof. Daniel Khomskii for his careful reading of the manuscript. The research leading to these results has received funding from the European Research Council under the EU Seventh Framework Programme (FP7/2007-2013) / ERC grant agreement n. 203523. Computational support from Caspur Supercomputing Center (Rome) is gratefully acknowledged.

-
- [1] M. Mostovoy and S.W. Cheong *Nature Mater* **6**, 13 (2007).
 - [2] T.Kimura, T. Goto, H. Shintani, K. Ishizaka, T. Arima, and Y. Tokura, *Nature* **426**, 55 (2003).
 - [3] D.V.Efremov, J. van der Brink, D. I. Khomskii, *Nat.Mater.* **3**, 853 (2004).
 - [4] S. Picozzi, I. A. Sergienko, K. Yamauchi, B. Sanyal and E. Dagotto, *Phys. Rev. Lett.* **77**, 227201 (2007).
 - [5] K. Yamauchi, S. Picozzi, *J. Phys. : Condens. Matter* **21**, 064203 (2009).
 - [6] N.Ikeda *et al.*, *Nature* **436**, 1136 (2005).
 - [7] D. Khomskii, *Bull. Am. Phys. Soc.* A13.00006 (2007); J. van den Brink and D. I. Khomskii *J. Phys.: Condens. Matter* **20** 434217 (2008)
 - [8] J. P. Wright *et. al*, *Phys. Rev. B* **66** (2002) 214422.
 - [9] J. Schlappa, *et al.* *Phys. Rev. Lett.* **100**, 026406 (2008).
 - [10] K. Kato, S. Iida, K. Yanai and K. Mizushima, *J. Magn. Mater.* **31-34**, 783 (1983).
 - [11] C. Medrano, M. Schlenker, J. Baruchel, J. Espeso, Y. Miyamoto, *Phys. Rev. B* **59**, 1185 (1999).
 - [12] P. W. Anderson, *Phys. Rev.* **102** (1956) 1008.
 - [13] P. Piekarz, K.Parlinski, and A. M. Oleś, *Phys. Rev. B* **66** (2002) 214422.
 - [14] I. Leonov, A. N. Yaresko, V. N. Antonov, M. A. Korotin, and V. I. Anisimov, *Phys. Rev. Lett.* **93**, 146404 (2004).
 - [15] H.-T. Jeng *et. al*, *Phys. Rev. Lett.* **93** (2004) 156403.
 - [16] H.-T. Jeng *et. al*, *Phys. Rev. B* **74** (2006) 195115.
 - [17] Y. Joly, J. E. Lorenzo, E. Nazarenko, J.-L. Hodeau, D. Mannix, and C. Marin, *Phys. Rev. B* **78**, 134110 (2008).
 - [18] A. Yanase and N. Hamada, *J. Phys. Soc. Japan* **68**, 1607 (1999).
 - [19] J.P. Wright, P. Attfield and P. G. Radaelli, *Phys. Rev. Lett.* **87**, 266401 (2004).
 - [20] J. M. Zuo, J. C. H. Spence, W. Petuskey, *Phys. Rev. B* **42** (1990) 8451.
 - [21] M. Alexe, M. Ziese, D. Hesse, P. Esquinazi, K. Yamauchi, T. Fukushima, S. Picozzi and U. Gösele, unpublished.
 - [22] Y. Miyamoto and M. Shindo, *J. Phys. Soc. Japan* **62**, 1423 (1993).
 - [23] G.Kresse and J.Furthmüller, *Phys.Rev.B* **54**, 11169 (1996).
 - [24] J.P.Perdew, K.Burke, and M. Ernzerhof, *Phys.Rev.Lett.* **77**, 3865 (1996)
 - [25] V.I.Anisimov, F.Aryasetiawan and A.I.Lichtenstein, *J. Phys.: Cond. Mat.* **9**, 767 (1997).
 - [26] R.D.King-Smith and D.Vanderbilt, *Phys. Rev. B* **47**, 1651 (1993); R. Resta, *Rev. Mod. Phys* **66**, 899 (1994).
 - [27] At variance with monotonous increase of P_x vs λ , P_z shows a bump at $\lambda \sim 0.5$ and decreases up to $\lambda = 1.0$: this trend may come from partial cancellation of ionic and electronic contribution to \mathbf{P} for $0.5 < \lambda < 1$.